

---

## Measurement of high energy $^3\text{He}$ in cosmic rays by the CAPRICE98 balloon experiment

---

E. Mocchiutti<sup>1\*</sup> for the WiZard/CAPRICE collaboration<sup>2</sup>

(1) *Royal Institute of Technology, Stockholm, Sweden*

(2) *see E. Mocchiutti et al., “Composition of cosmic ray particles in the atmosphere as measured by the CAPRICE98 balloon borne apparatus”, in this proc.*

\* E-mail: mocchiut@particle.kth.se

---

### Abstract

We report the first measurement above 5 GeV/n of the  $^3\text{He}$  component in the cosmic rays. The CAPRICE98 apparatus was flown on 28–29 May 1998 and was equipped with a gas RICH detector, a silicon–tungsten calorimeter and a time of flight system. By combining the RICH and the spectrometer information it was possible to separate  $^3\text{He}$  from  $^4\text{He}$  in the rigidity range from 26 to 30 GV. In this paper we describe the analysis and report on the  $^3\text{He}$  flux and the  $^3\text{He}/^4\text{He}$  ratio in the kinetic energy range 16.4 to 19.1 GeV/n.

### 1. Introduction

$^3\text{He}$  and deuterium are very fragile isotopes, destroyed rather than formed in the stars. Their presence in the cosmic rays is due to the spallation of cosmic rays  $^4\text{He}$ . Since they are stable nuclei they provide information on the mean amount of matter traversed by the cosmic rays before escaping from the Galaxy.

Unlike heavier secondary nuclei, such as Li, Be and B,  $^3\text{He}$  and deuterium interaction mean free path is considerably larger than the escape mean free path from the Galaxy. Hence they are ideal probes to study cosmic ray propagation in the whole containment volume.

### 2. The CAPRICE98 experiment

The balloon–borne CAPRICE98 detector was flown from Ft. Sumner, New Mexico, USA on May 28–29, 1998 at a vertical rigidity cutoff of about 4.3 GV. The data analyzed for this work were collected at an average atmospheric depth of about 5.5 g/cm<sup>2</sup> with an exposure time of almost 21 hours.

The apparatus consisted of a superconducting magnet spectrometer, a time–of–flight device, a gas ring imaging Cherenkov detector (RICH) and a silicon–tungsten imaging calorimeter. More details on the instrumental setup and capabilities of this experiment can be found in previous publications (i.e. [1]).

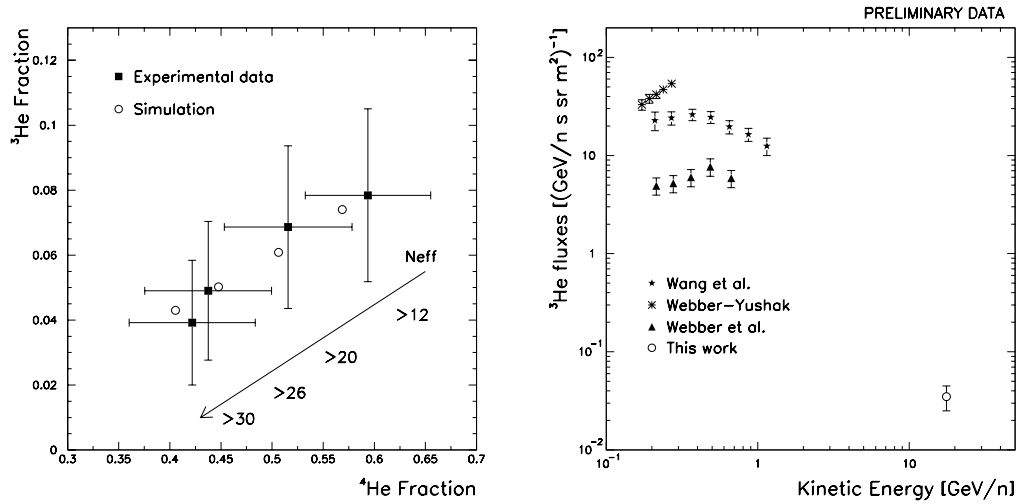


**Fig. 1.** On the left: comparison between simulation and real data. On the right: measured  $^3\text{He}$  fluxes compared with present results above  $0.1 \text{ GeV}/n$  [13,14,15].

### 3. Data analysis

Charge two particles can be reliably identified in the CAPRICE98 apparatus by using the pulse-height information from the time-of-flight scintillators (see [4] for selection and selection efficiencies).

The  $^3\text{He}$  threshold for emitting light in the RICH was 26.4 GV while the  $^4\text{He}$  threshold was 35.1 GV. Because of the tracker resolution and of the RICH resolution, it was possible to separate  $^3\text{He}$  from  $^4\text{He}$  in the rigidity bin from 26 to 30 GV using the RICH as a threshold device.

A strong selection was used by requiring the number of pads used in the reconstruction of the Cherenkov angle ( $N_{eff}$ ) to be greater than 26. This selection resulted in a negligible contamination due to the noise in the RICH multi-wire proportional chamber and reduced strongly the contamination of  $^4\text{He}$  events just above threshold with the wrongly reconstructed rigidity. The  $^4\text{He}$  contamination was further reduced by applying strong conditions on the tracking system.

To determine the  $^3\text{He}$  efficiency and  $^4\text{He}$  contamination a simulation was used. The resolution functions of the RICH and of the spectrometer used in the simulation were first obtained from charge one particles at ground and then scaled for charge two particles in the flight conditions. The simulation was checked by a comparison of variables obtained from the simulation with the correspondent experimental ones; as an example Fig. 1 on the left compares simulated and experimental fractions of  $^3\text{He}$  and  $^4\text{He}$  just above threshold. Different cuts on  $N_{eff}$  are reported. Errors of the simulated data are included in the points. The

**Table 1.** Preliminary selection efficiency and contamination.

Energy bin [GV]	Charge 2 events	Selected ${}^3\text{He}$ events	${}^3\text{He}$ efficiency ( $N_{eff} > 26$ )	Contamination ${}^4\text{He}_{sel}/({}^4\text{He}_{sel}+{}^3\text{He}_{sel})$
26 – 30	102	7	0.37	0.15

**Table 2.** Preliminary  ${}^3\text{He}$  fluxes at the Top Of the Atmosphere (TOA).

Energy bin [GeV/n]	Mean value	Flux at TOA [(GeV/n s sr m <sup>2</sup> ) <sup>-1</sup> ]	${}^3\text{He}/{}^4\text{He}$ ratio
16.4 – 19.1	17.6	$0.035 \pm 0.010$	$0.18 \pm 0.05$

two fractions in this figure were calculated in the bin from 26 to 30 GV in the case of  ${}^3\text{He}$  and in the bin from 35 to 39 GV for  ${}^4\text{He}$ . In both cases the selected number of events obtained by asking  $N_{eff}$  greater than the numbers reported in figure was then divided by the total number of charge two particles in that energy bin. Hence this procedure, identical in the experimental and simulated case, calculates these fraction assuming no contamination in both the  ${}^3\text{He}$  and  ${}^4\text{He}$  samples. A good agreement was found between simulated and experimental data.

Hence the final selection efficiency and contamination used in the analysis were obtain from the simulation using pure samples of  ${}^3\text{He}$  and  ${}^4\text{He}$ .

The secondary  ${}^3\text{He}$  component [12] was subtracted in order to obtain the flux at the top of the atmosphere.

#### 4. Results and discussion

Tables 1 and 2 report preliminary results of efficiency, contamination and fluxes. Fig. 1 on the right reports the measured  ${}^3\text{He}$  flux while Fig. 2 reports the  ${}^3\text{He}$  to  ${}^4\text{He}$  ratio obtained in this work ( ${}^4\text{He}$  data from [4]) together with other experimental results; in the latter also shown are the theoretical prediction of the Leaky Box Model (LBM) [10], the Nested Leaky Box Model (NLBM) [5], the Thick Source Model (TSM) [6] and the Close Galaxy Model (CGM) [8].

Results from the CAPRICE98 experiment seems to better support the CGM and TSM models than the LBM and NLBM models reported [5,10]. Notice that deuteron CAPRICE98 measurement support the same models [2], even if it is compatible with different calculation for the LBM [11].

#### 5. References

1. Ambriola M. et al. 1999, Nucl. Phys. B (Proc. Suppl.), 78, 32.

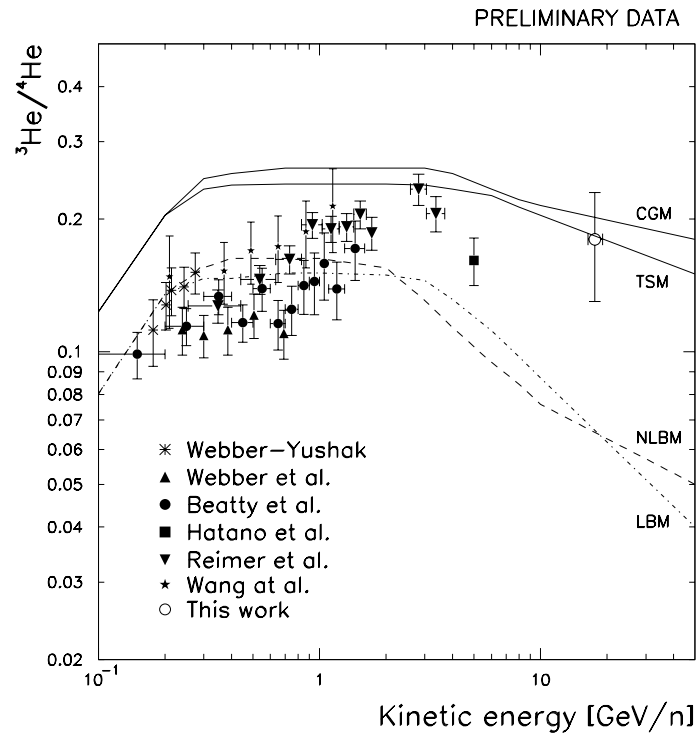


**Fig. 2.**  ${}^3\text{He}$  to  ${}^4\text{He}$  ratio. Also shown are data from other experiments [3,7,9,13,14,15] and theoretical prediction as explained in the text.

2. Ambriola M. et al 2002, Nucl. Phys. Proc. Suppl., 113:88-94.
3. Beatty J. J. et al. 1993, Astrphys. Jour., 413, 268.
4. Boezio M. et al. 2003, Astrop. Phys, to appear, astro-ph/0212253.
5. Cowsik R. & Gaisser T. K. 1973, Proc. ICRC 13<sup>th</sup>, 1, 500.
6. Cowsik R. & Gaisser T. K. 1981, Proc. ICRC 17<sup>th</sup>, 2, 218.
7. Hatano Y. et al. 1995, Phys. Rev. D, 52, 6219.
8. Peters B. & Westergaard N. J. 1977, Astrphys. Sp. Sci., 48, 21.
9. Reimer O. et al. 1998, Astrphys. Jour., 496, 490.
10. Stephens S. A. 1989, Adv. Sp. Res., 9, 145.
11. Vannuccini E. et al. 2003, "Measurement of the deuterium flux in the kinetic energy range 12–22 GeV/n with the CAPRICE98 experiment", this Proc.
12. Vannuccini E. 2003, private communication and Vannuccini E., Papini P., Grimani C. and Stephens S. A. 2001, Proc. ICRC 27<sup>th</sup>, 10, 4181.
13. Wang J. Z. et al. 2002, Astrophys. Jour., 564, 244.
14. Webber W. R. et al. 1991, Astrophys. Jour., 380, 230.
15. Webber W. R. & Yushak 1983, Astrphys. Jour., 275, 391.